Supplementary Information

Cancer-Microenvironment-Sensitive Activatable Quantum Dot Probe in the Second Near-Infrared Window

*Sanghwa Jeong[†], Jaejung Song[‡], Wonseok Lee[†], Yeon Mi Ryu[§], Yebin Jung[†], Sang-Yeob Kim[§,#], Kangwook Kim[†,¶], Seong Cheol Hong[†], Seung Jae Myung[§,#,⊥], Sungjee Kim[†,‡]**

[†]Department of Chemistry, Pohang University of Science and Technology (POSTECH), San 31, Hyojadong, Nam-gu, Pohang 37673, South Korea

[‡]School of Interdisciplinary Bioscience and Bioengineering, Pohang University of Science & Technology (POSTECH), San 31, Hyojadong, Namgu, Pohang 37673, South Korea

[§]Asan Institute for Life Sciences, Asan Medical Center, 88 Olympic-ro, 43-gil, Songpa-gu, Seoul, 05505, Republic of Korea

[#]Department of Convergence Medicine, University of Ulsan College of Medicine, 88 Olympic-ro, 43-gil, Songpa-gu, Seoul 05505, Republic of Korea

[¶]Department of Civil and Environmental Engineering, Korea Army Academy at Young-cheon, Yeongcheon-si, Gyeongsangbuk-do, South Korea

[⊥]Department of Gastroenterology, Asan Medical Center, University of Ulsan College of Medicine, 88 Olympic-ro, 43-gil, Songpa-gu, Seoul, 05505, Republic of Korea

1. Synthesis of PbS/CdS/ZnS core/shell/shell QDs

1.1 Materials

Lead(II) acetate trihydrate, cadmium acetate hydrate, zinc oxide, octadecene (ODE) (technical grade, 90%), bis(trimethylsilyl)sulfide ($(TMS)_2S$) (synthesis grade), trioctylphosphine (TOP) (technical grade, 90%), and oleic acid (OA) (technical grade, 90%), lipoic acid, sodium borohydride, 1-Ethyl-3-(3-(dimethylamino)propyl)carbodiimide (EDC) and N-hydroxysulfosuccinimide sodium salt (S-NHS) were all purchased from Sigma-Aldrich. All chemicals were used without further purification.

1.2 Synthesis of PbS QDs

All manipulations were performed using the standard air-free Schlenk line technique. We modified the Hines' method to synthesize PbS QDs.[1] In a typical synthesis of ~7.5-nm-sized PbS QDs, the lead precursor solution was prepared as follows: lead(II) acetate trihydrate (4 mmol) was suspended in a mixture of OA (20 mL) and ODE (20 mL) and degassed for 30 min under vacuum at 100 °C. The solution was then heated to 180 °C for 1 h under a N_2 atmosphere. After the solution became transparent, it was cooled to 100 °C and degassed for 30 min. The sulfur precursor solution was prepared as follows: sulfur (15 mmol) in ODE (15 mL) was degassed at 100 °C for 30 min, and then heated to 180 °C for 1 h under a N_2 atmosphere. After the solution turned red, it was cooled to room temperature. Following this, the sulfur solution (3.2 mL) was mixed with $(TMS)_2S$ (0.8 mmol) and ODE (16.8 mL) under a N_2 atmosphere to complete the preparation of the sulfur precursor solution. The lead precursor solution was heated to 175 °C under a N_2 atmosphere and sulfur precursor solution was quickly injected into the lead precursor solution. The temperature was maintained for 1

min. The reaction was quenched by the quick injection of cold toluene (20 mL) and TOP (4 mL). The size of the QDs could be tuned by controlling the temperature at which sulfur precursor solution was injected. The final product solution was purified before characterization and device fabrication by centrifugation with the addition of methanol. The black precipitate acquired after centrifugation was washed with methanol three times and re-dispersed in hexane. The QD precipitates were dispersed in tetrachloroethene to measure the absorption and photoluminescence spectra.

1.3 Cation exchange from PbS QDs to PbS/CdS core/shell QDs

The cation exchange process for thick-shell CdS on PbS QDs was based on Zhao et al.'s method[2] with slight modification. A 0.2 M cadmium oleate solution was prepared by heating a mixture of CdO (6 mmol), OA (9 mL, 24 mmol), and ODE (20 mL) to 255 °C under a nitrogen purge until all of the CdO had dissolved. The clear solution was cooled to 100 °C under nitrogen gas atmosphere and degassed under vacuum to remove residual water molecules. Purified PbS QDs (200 nmol) were dispersed in ODE (35 mL), degassed under vacuum at room temperature, and added to a 5 mL aliquot of the 0.2 M cadmium oleate solution ([Cd]/[QD] ≈ 10k). The solution was slowly heated to 100 °C under a nitrogen atmosphere and held at this temperature for 1 h. After thin CdS shell formation at 100 °C, the temperature of the solution was increased to 150 °C and maintained for 10 min, and then further increased to 200 °C for 10 min. Finally, the temperature was raised to 240 °C and maintained for 20 min. Subsequently, the reaction flask was cooled to room temperature. An aliquot of known volume was extracted and diluted in toluene to calculate the extinction coefficient of PbS/CdS QDs on the basis of the number of exploited PbS QDs. The PbS/CdS QD solution was precipitated and purified by centrifugation with methanol, acetone, and

toluene (crude solution:toluene:methanol:acetone=2:3:30:10 (v/v%)). The dark-yellow precipitates acquired after centrifugation was washed with methanol 3 times. The purification step was replayed at least two times to remove unreacted precursors.

1.4 ZnS shell overcoating on PbS/CdS core/shell QDs

Synthesis of zinc precursor (0.5 M): The zinc precursor solution was prepared by dissolving ZnO (7.5 mmol) in OA (9.5 mL) and ODE (5.5 mL). The mixture was degassed at 100 °C under vacuum for 30 min, and then heated to 200 °C for 1 h. The transparent viscous solution was cooled to 100 °C and degassed under vacuum. The precursor solution was kept at 140 °C in nitrogen atmosphere.

Synthesis of sulfur precursor (0.5 M): The sulfur precursor solution was prepared as follows: sulfur (7.5 mmol) in ODE (15 mL) was degassed at 100 °C for 30 min, and then heated to 180 °C for 1 h under a nitrogen atmosphere. After the solution turned to red, it was cooled down to 100 °C.

Overcoating of ZnS shell: PbS/CdS QDs (60 nmol) were injected into ODE (12 mL) in a 50 mL three-neck round bottom flask. The solution was degassed at 100 °C for 30 min under vacuum with magnetic stirring. The solution was further heated to 240 °C under a nitrogen atmosphere for 20 min. Typically, the zinc precursor solution (140 μL), which was calculated for a monolayer of ZnS on PbS/CdS QDs (diameter ≈ 7.5 nm), was injected using a glass syringe and the temperature was maintained for 5 min. Subsequently, the sulfur precursor solution (140 μL) was injected using a glass syringe and the temperature was maintained for an additional 5 min. Similar to the SILAR method, the sequential injection of zinc and sulfur precursors was repeated two times (giving a total of three injection steps for each zinc and

sulfur precursor). The product solution was cooled to room temperature 5 min after the final injection of the sulfur precursor. The final product was precipitated and purified by centrifugation with methanol, acetone, and toluene (crude solution:toluene:methanol:acetone=2:3:30:10 (v/v%)). The dark-yellow precipitates acquired after centrifugation was washed with methanol 3 times. The purification step was replayed at least two times to remove unused precursors.

2. Ligand exchange of NIR-II emitting QDs

The surfactants of crude QDs including PbS/CdS/ZnS QDs (NIRQD), PbS/7CdS QDs, PbS/7CdS QDs, and PbS QDs as defined in manuscript—were exchanged from OA to hydrophilic ligands. The ligand exchange was conducted by using LA. A 10^5-fold excess of the ligand was used. To reduce the disulfide bond of LA to yield dihydrogen lipoic acid (DHLA), LA (1 mmol) in deionized water (2 mL) was reduced by the addition of sodium borohydride (2.2 equiv.) followed by vigorous stirring for 20 min at room temperature. The purified QDs (10 nmol) in 1 mL chloroform were mixed with the solution of DHLAs and stirred vigorously for 1 hours at 50 °C. During the surfactant exchange, the QDs were transferred from chloroform to the aqueous phase. After ligand exchange, the aqueous phase was separated and degassed at room temperature under vacuum to remove residual chloroform. The QD aqueous solution was filtered with a 0.2 μm membrane filter to remove aggregates. To remove any excess ligand, the QD solution was dialyzed using Amicon 50 kDa MW cutoff centrifugal filters.

3. Measurement of photoluminescene quantum yield of QD

Photoluminescence quantum yield (PL QY) of NIR-II emitting QDs were calculated relative to NIR-II fluorescent Dye 26 (Acros) which has been most widely used for relative PL QY measurement in NIR-II region. Note that the PL QY of IR-26 in 1,2-dichloroethane has been the subject of dispute, with reported values between 0.5%[3] and 0.05%.[4,5] The wide variation in the PL QY of the reference dye can make a 10-fold difference in the sample PL QY. In this paper, a PL QY of 0.05% was used as the reference QY for IR-26 based on recent studies describing absolute PL QY measurement using an integrating sphere.[4,5] The PL QY of the QDs were calculated using the following equation.

$$\phi_{QD} = \phi_{Ref} \times \frac{Fluorescence(QD)}{Fluorescence(Ref)} \times \frac{Absorbance(Ref)}{Absorbance(QD)} \times \frac{n_{QD}^2}{n_{Ref}^2}$$

where Φ_{QD} is the PL QY of the QD, Φ_{Ref} is the PL QY of the reference dye, *Absorbance* is the absorbance at the excitation wavelength, and *n* is the refractive index of the solvent. The absorbance of both the QDs and the reference dye was optimally maintained between 0.01 and 0.05 to ensure low reabsorption. The PL QYs of NIR-II QDs in aqueous solutions are known to be affected by cuvette shape (i.e., path length) owing to differences in the amount of water solvent-absorbing NIR-II light. In this study, a micro cell (light path 10 mm × 2 mm, 104.002F-QS, Hellma) was used as the cuvette for the PL QY measurement.

4. Calculation of band energy level in NIRQDs

The conduction and valence energy levels of NIRQDs were calculated to investigate the driving force behind the photoexcited electron transfer (PET) (Figure S3). Alternatively, the band-edge emission peak of NIRQDs in the NIR-II region was exploited to calculate the band gap energy of the core PbS QDs since the PbS/CdS/ZnS QDs did not show a distinct first excitonic absorption peak because of their heterogeneous core size. The conduction and valence band levels of PbS core in the NIRQD were estimated as -4.2 and -5.3 eV,

respectively, by a simple quantum confinement effect calculation based on the NIRQD emission wavelength.[6] Methylene blue (MB) has a LUMO level positioned at −4.55 eV relative to the vacuum level.[7,8] MB LUMO is located below the conduction level of PbS, which is well suited for the transfer of photoexcited electrons from the PbS core to MBs on the surface. The CdS shells are thick, and thus, bulk energy levels can be safely assumed.

5. Preparation of protease-activatable NIRQD (PA-NIRQD)

Fabrication of activatable modulator (AcM): All peptide sequences were purchased from Peptron, Daejeon, Republic of Korea. The peptide sequence—which included an MMP-cleavable peptide sequence (–PLVGR–) for PA-NIRQD, having the peptide structure PEG_8–GGPLGVRGGCDDDD (AcM-noMB, where PEG_8 = a tetramer of 8-amino-3,6-dioxaoctanoic acid)—was reacted with maleimide-modified methylene blue (mi-MB). mi-MB was purchased from ATTO-Tec, Germany. Peptide sequence and maleimide can be conjugated by the formation of thioester bond between maleimide and thiol group of cystein. Before conjugation, mi-MB and AcM-noMB were dissolved in DMSO and filtered deionized water, respectively. AcM-noMB was mixed with concentrated mi-MB in the ratio AcM-noMB:mi-MB = 1.3:1 (mol%) in 20 mM 4-(2-hydroxyethyl)-1-piperazineethanesulfonic acid (HEPES) buffer at pH 7.0. The reaction solution was vortexed vigorously for 4 hours in room temperature. The final product was purified by size exclusion chromatography (molecular weight cutoff = 700 Da, GE Healthcare Sephadex G-10) to yield the pure AcM, which was stored in 4 °C. The peptide sequences for control experiments was also reacted with mi-MB by the same fashion. (AcM-noAsP: PEG_8-GGPLGVRGC-MB, AcM-DD: PEG_8-GGPLGVRG(-MB)CDD, AcM-noPEG: GGPLGVRG(C-MB)DDDD)

Fabrication of PA-NIRQD using AcM and NIRQD: AcM was conjugated with NIRQDs coated with the mixed ligands of DHLA and zw-DHLA ligands using the simple amide bond formation chemistry between carboxylic group of DHLA and *N*-terminal amine group of AcM. First, the NIRQD aqueous solution was sufficiently dialyzed to remove excess ligands and concentrated to >5 μM. EDC (200 equivalents relative to the QDs) and Sulfo-NHS (400 equivalents relative to QDs) were added to the NIRQD solution in 20 mM 2-(*N*-morpholino)ethanesulfonic acid buffer at pH 6.5. After 20 min of vortexing, the excess EDC and Sulfo-NHS were sequentially dialyzed using MES buffer at pH 6.5 and deionized water with Amicon 50 kDa MW cutoff centrifugal filters. Finally, the desirable amounts of AcMs in 100 mM phosphate buffer solution (PBS) at pH 7.4 was added to the EDC/S-NHS-activated NIRQD solution. A final volume of less than 100 μL was used to ensure high reaction yields. The reaction solution was incubated for 2 h at room temperature on a shaker. After conjugation, the complex between NIRQD and AcM (PA-NIRQD) was purified using filtered deionized water and a 50 kDa centrifugal filter to eliminate excess AcMs. To detach the undesirably bound AcMs on the surface of NIRQDs without amide bond formation, PA-NIRQD solution was treated by the addition of 10^4 equimolar amounts of mixed ligands of DHLA and zw-DHLA to PA-NIRQDs (DHLA:zw-DHLA=1:1). The 0.5 M mixed ligand solution was reduced with sodium borohydride using the same method described for the surface modification of NIRQDs, and injected into PA-NIRQDs (10 μmol of mixed ligands to 1 nmol of PA-NIRQDs). The mixture was gently vortexed for 1 h at room temperature and sufficiently dialyzed with filtered deionized water to separate the mixed ligands and unconjugated AcMs from PA-NIRQD. The final product was stored at 4 °C. With the exception of the comparison study involving PA-NIRQD, PA-NIRQD-DD, and PA-NIRQD-noAsp, a nominal ratio of 40 AcMs to 1 NIRQD was typically used for further experiments; in the case of the comparison study, the ratio of modulators to NIRQD was 12:1.

6. Fluorescence activation of PA-NIRQD by proteolytic cleavage

For cleavage using MMP-2, PA-NIRQD (50 μL of 200 nM) in MMP-2 buffer (20 mM Tris buffer with 50 mM NaCl, 0.1 mM $CaCl_2$, and 20 mM $Zn(NO_3)_2$ at pH 7.5) was prepared. Additionally, MMP-2 catalytic domain (50 μL of 20 μg/mL; Enzo Life Sciences, BML-SE237-0010) in MMP-2 buffer was prepared without a further activation step and mixed with the PA-NIRQD solutions. The final MMP-2 concentrations were 10, 20, and 30 μg/mL. The change in fluorescence was recorded using a HORIBA Jobin Yvon Fluorolog3 InGaAs CCD, which uses a Xe lamp with an excitation wavelength of 828 nm. In a control experiment, the global MMP inhibitor *N*-isobutyl-*N*-(4-methoxyphenylsulfonyl)glycyl hydroxamic acid (10 μM; Enzo Life Sciences, BML-PI115-0025) was co-incubated with the MMP-2 catalytic domain (10 μg/mL) for 30 min before being mixed with the PA-NIRQD solution.

7. Cell viability test

Hela, HT29, and CCT841 cells were seeded in 96-well plates (104 cells/well; Corning) and incubated for 1 day at 37°C under 5% CO_2. The cells were then treated with PA-NIRQD samples under dark conditions. The concentrations of these agents were equivalent to 200, 400 nM, and 1 μM, respectively. The samples were incubated for 1, 6, 12, or 24 h at 37°C under 5% CO_2. At the end of each incubation time, Cell Counting Kit-8 solution (CCK-8, Dojindo Laboratories) was added to the samples according to the manufacturer's instructions. After 2 h of incubation, the absorbance at 450 nm was measured using a microplate reader. The measurement results were expressed as the ratio between the absorbance of the sample and that of the negative control cells, which had not experienced sample incubation.

8. Toxicity of PA-NIRQDs in mice

Twelve 6-week-old male BALB/c mice were randomly assigned into two groups of six mice. Mice in experimental group were intravenously injected with 0.1 nmol PA-NIRQD in 100 μL PBS buffer, while the mice in control group were injected with 100 μL PBS only. The mice were weighed and their behaviors were evaluated daily. Seven days after treatment, the mice were anesthetized, and then sacrificed by cervical dislocation. Blood samples were harvested for the measurement of hematological parameters (ADVIA® 120 Hematology System) and of biochemical markers for kidney and liver functions (Hitachi 7180 autoanalyser; Hitachi High-Technologies Corp., Tokyo, Japan).

9. Preparation of AOM/DSS mouse model

Four week male BALB/c mice (Charles River Laboratories Japan, Inc., Yokohama, Japan) were acclimatized to tap water and an ad libitum basal diet for 7 days. The mice were given a single intraperitoneal injection of azoxymethane (AOM; 10 mg/kg body weight; Sigma-Aldrich). One week later, the animals were administered 2% (w/v) dextran sulfate sodium (DSS; molecular weight 36,000-50,000) for 7 days via drinking water, followed by maintenance on a basal diet and tap water for 14 days. This DSS administration via drinking water was repeated. Colonoscopy (Karl Storz, Tuttlingen, Germany) was performed in an AOM/DSS model to check whether colon tumors were adequately formed. The mice were sacrificed at 4 weeks after the completion of DSS administration. All animal experiments were performed with protocols approved by the Institutional Animal Care and Use Committee (IACUC) of the Asan Institute for Life Sciences at the Asan Medical Center, consistent with the Institute of Laboratory Animal Resources (ILAR) guide. The colons of AOM/DSS treated mice were removed, flushed with PBS, and dissected longitudinally.

10. *Ex Vivo* mouse colon tissue fluorescence imaging by spraying PA-NIRQD

Fresh intact colon tissues were obtained from AOM/DSS mouse model by surgical excision and longitudinally cutting to expose the mucosa layer of colon immediately after the sacrifice. The colon tissue was placed onto a glass substrate at room temperature. The fresh colon tissues were sprayed by 1 μM PA-NIRQD probe in a 100 mM PBS solution at pH 7.4. The probe solution was sprayed using micropipettes by rapidly ejecting small portions of the probe solution to evenly coat the colon mucosal layer surfaces that had been longitudinally cut. Then, 50–100 μL of the probe solution was used in a single experiment. After 1 min of spraying, any spilled solution present on the colon tissue was removed. The colon tissues were placed on a temperature-controlled stage at room temperature with the mucosal layer facing up and brought into the NIR-II fluorescence imaging system. The stage temperature was increased to 38 °C and fluorescence imaging was started. NIR-II fluorescence reflectance imaging was performed on a home-built imaging system with thermoelectrically cooled SC-2500 InGaAs CCD camera (FLIR, France). The colon tissues were excited with a 200 mW/cm^2, 910 nm pulse laser. To reduce the exposure to laser energy, the irradiation was temporally controlled using a home-built program such that it was activated only during image capture. The emitted photons were collected with integration time of 100 ms through a 1000-nm long pass filter. As a negative control group, normal NIRQDs were sprayed onto colon cancer models using the method described above. A second negative control group was obtained by spraying PA-NIRQD onto the normal colon using the method described above; in this case, the colon tissue was prepared from a normal mouse (male BALB/c, Charles River Laboratories Japan, Inc., Yokohama, Japan).

For the tissue phantom study of NIR-I, the tumor region on untreated colon cancer tissue was sprayed with 5 mg/mL Genhence 750 (Perkin Elmer) in 100 mM PBS buffer at pH 7.4. Colon cancer tissues sprayed by PA-NIRQD were exploited for NIR-II sample. NIR-I

fluorescence reflectance imaging was performed on the home-built setup with Orca-ER Si CCD camera (Hamamatsu). The colon tissue was excited with light of 660 nm, at 10 mW/cm^2, and the emitted photons were collected with integration time of 100 ms through an 800-nm band-pass filter. NIR-II fluorescence imaging was conducted in the typical manner. The colon tissues were placed on the bottom of cylindrical container and covered with thin (<0.1 mm) polyethylene film, transparent in NIR-I and NIR-II, to prevent the dissolution of fluorescent probes. A liquid tissue phantom solution was prepared by the dilution of intralipid solution (Intralipid 20% emulsion, Sigma-Aldrich) to a final concentration of 1% intralipid aqueous solution. The fluorescence images were measured with increasing the thickness of liquid phantom over the tissue from 0 mm to 5 mm.

11. Characterization

UV–Vis absorption spectra were measured using a Hewlett-Packard Agilent 8453 spectrophotometer. The change in fluorescence was recorded using a HORIBA Jobin Yvon Fluorolog3 InGaAs CCD, which uses a Xe lamp with an excitation wavelength of 828 nm. TEM images were obtained using JEOL JEM-2100. Scanning TEM (STEM) and STEM-high-angle annular dark field (STEM-HAADF) was conducted using JEOL JEM-ARM200F. X-ray diffraction patterns were collected with a RIGAKU JAPAN D/MAX-2500/PC diffractometer. Hydrodynamic size and zeta potential of colloidal nanoparticles were gathered using Malvern zetasizer Z and S. Mass spectroscopy data were obtained at eMass, Seoul, Republic of Korea, using the matrix-assisted laser desorption/ionization time-of-flight method.

1. Hines, M.A. & Scholes, G.D. Colloidal PbS nanocrystals with size-tunable near-infrared emission: Observation of post-synthesis self-narrowing of the particle size distribution. *Adv. Mater.* **15**, 1844-1849 (2003).

2. Zhao, H., Chaker, M., Wu, N. & Ma, D. Towards controlled synthesis and better understanding of highly luminescent PbS/CdS core/shell quantum dots. *J. Mater. Chem.* **21**, 8898-8904 (2011).

3. Zhang, Y. et al. Ag_2S Quantum Dot: A Bright and Biocompatible Fluorescent Nanoprobe in the Second Near-Infrared Window. *ACS Nano* **6**, 3695-3702 (2012).

4. Semonin, O.E. et al. Absolute Photoluminescence Quantum Yields of IR-26 Dye, PbS, and PbSe Quantum Dots. *J. Phys. Chem. Lett.* **1**, 2445-2450 (2010).

5. Hatami, S. et al. Absolute photoluminescence quantum yields of IR26 and IR-emissive $Cd_{1-x}Hg_xTe$ and PbS quantum dots - method- and material-inherent challenges. *Nanoscale* **7**, 133-143 (2015).

6. McDonald, S.A. et al. Solution-processed PbS quantum dot infrared photodetectors and photovoltaics. *Nat. Mater.* **4**, 138-142 (2005).

7. Shen, J.-S., Yu, T., Xie, J.-W. & Jiang, Y.-B. Photoluminescence of CdTe nanocrystals modulated by methylene blue and DNA. A label-free luminescent signaling nanohybrid platform. *Phys. Chem. Chem. Phys.* **11**, 5062-5069 (2009).

8. Yang, Y., Rodríguez-Córdoba, W. & Lian, T. Ultrafast Charge Separation and Recombination Dynamics in Lead Sulfide Quantum Dot–Methylene Blue Complexes Probed by Electron and Hole Intraband Transitions. *J. Am. Chem. Soc.* **133**, 9246-9249 (2011).

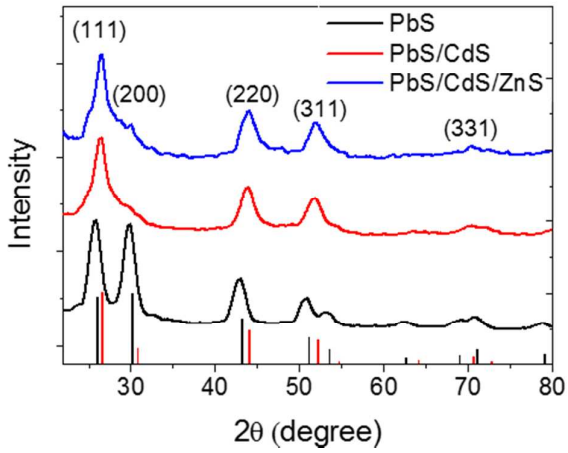

Figure S1. X-ray diffraction pattern of PbS, PbS/CdS, and PbS/CdS/ZnS QD powders. Vertical bars (bottom) correspond to reference data of the rock-salt cubic crystalline structure of PbS (black) and zinc blende structure of CdS (red) (JCPDS file No. 01-078-1054 and No. 10-454, respectively).

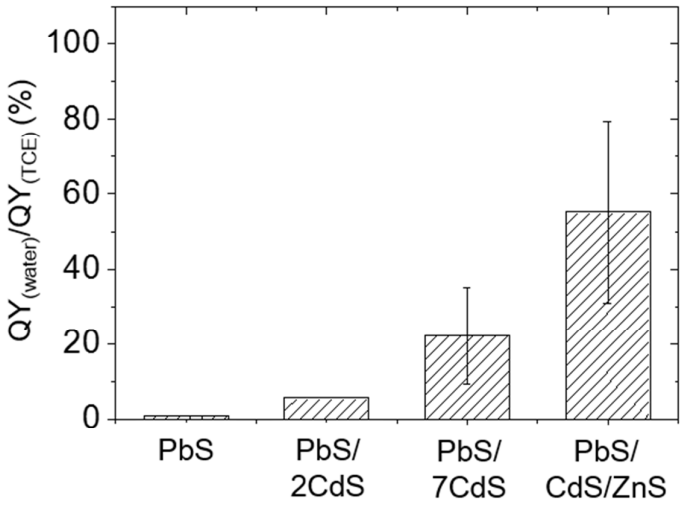

Figure S2. Comparison of relative PL QY of PbS QD, PbS/2CdS QD, PbS/7CdS QD, and PbS/CdS/ZnS QD (NIRQD) before and after direct ligand exchange with dihyrdolipoic acid (DHLA). The PbS cores and PbS/2CdS, PbS/7CdS, and PbS/7CdS/ZnS QDs were transferred to the aqueous phase via DHLA ligand exchange, and the PL QYs in water were compared with those in tetrachloroethylene. The average values from three different batches of PbS/7CdS QDs and PbS/7CdS/ZnS QDs were used; error bars show standard deviations.

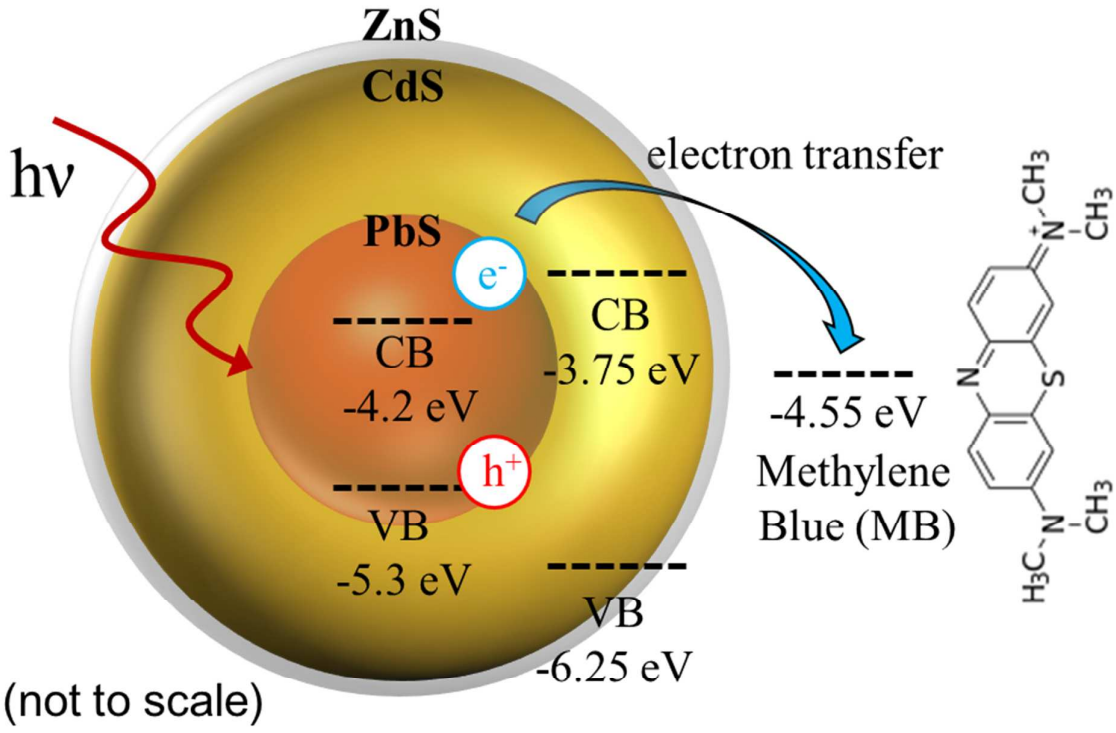

Figure S3. Schematic of photoexcited electron transfer from PbS/CdS/ZnS QDs to MB with the calculated energy level diagram. The conduction band (CB) and valence band (VB) of the ZnS shell are omitted due to the shell thinness. LUMO = lowest unoccupied molecular orbital. HOMO = highest occupied molecular orbital.

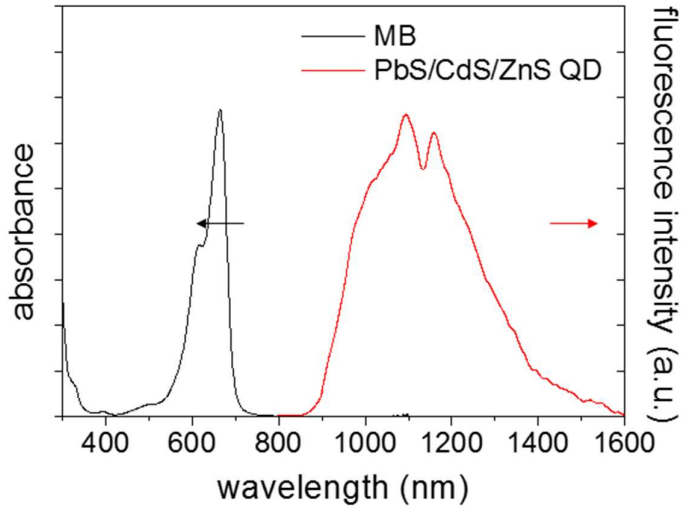

Figure S4. Absorption spectrum of MB in chloroform (black line) and fluorescence spectrum of PbS/CdS/ZnS QDs in toluene (red line). No spectral overlap is observed in the NIR-II region.

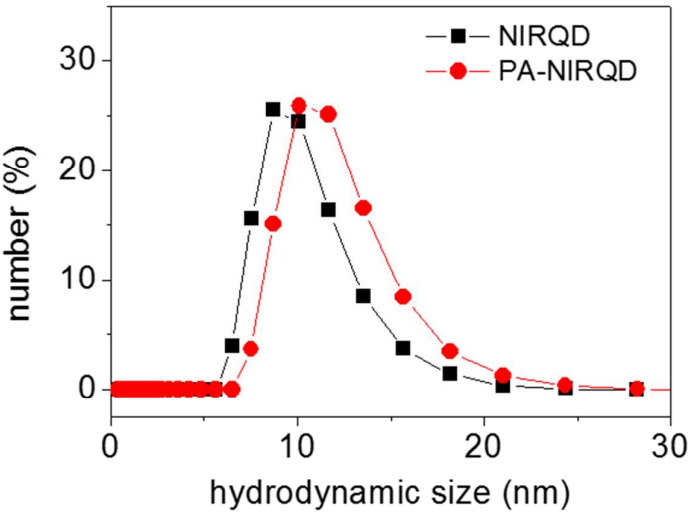

Figure S5. Dynamic light scattering histogram of the hydrodynamic (HD) size of NIRQD and PA-NIRQR conjugated with AcM (AcM/QD = 40). The average HD sizes are 10.0 and 11.7 nm for NIRQD and PA-NIRQD, respectively.

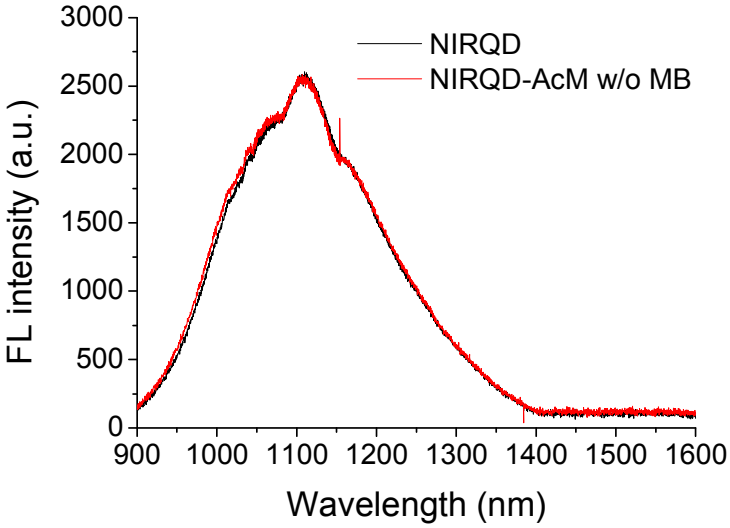

Figure S6. FL spectra of water-dispersed NIRQD solution and NIRQD conjugated by AcM without the MB quencher (NH_2-PEG_8-GGPLGVRGGCDDDD). The QD concentrations of the two samples are equal.

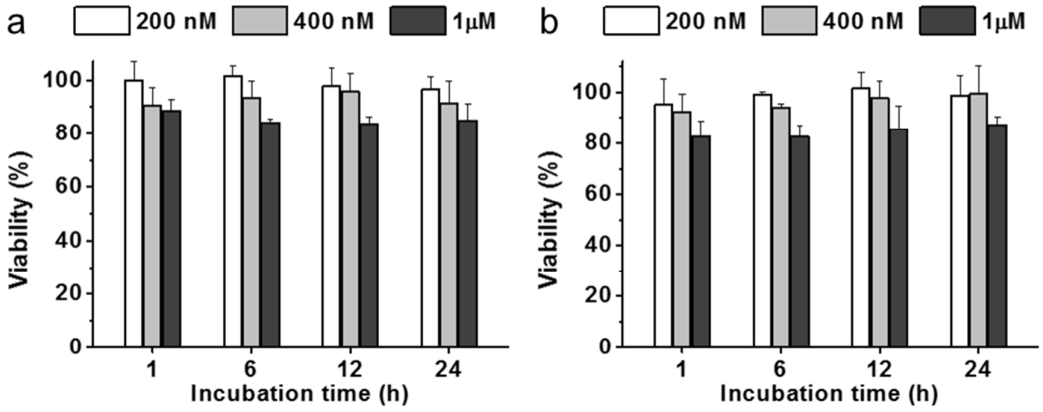

Figure S7. Cell viability test to evaluate the cytotoxicity of PA-NIRQD in (a) human colorectal adenocarcinoma (HT29) and (b) human colon (CCD 841) cells by cell counting kit-8 assay.

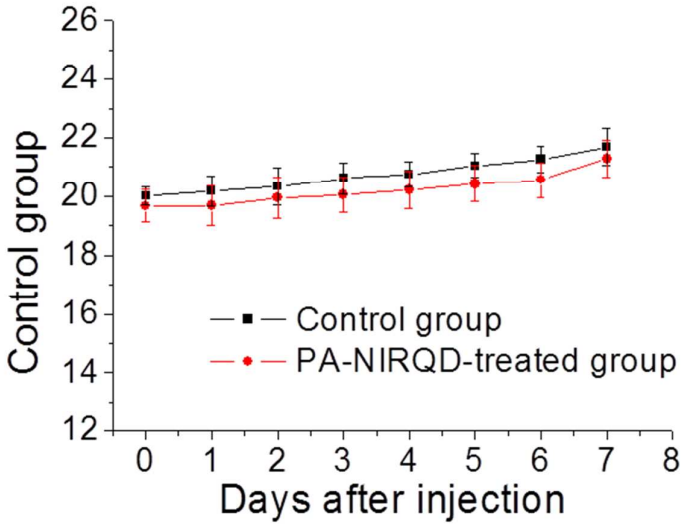

Figure S8. Body weight changes for the mice that were intravenously administered by PA-NIRQD and the control group over 7 days. There was no notable difference in weight between the two groups.

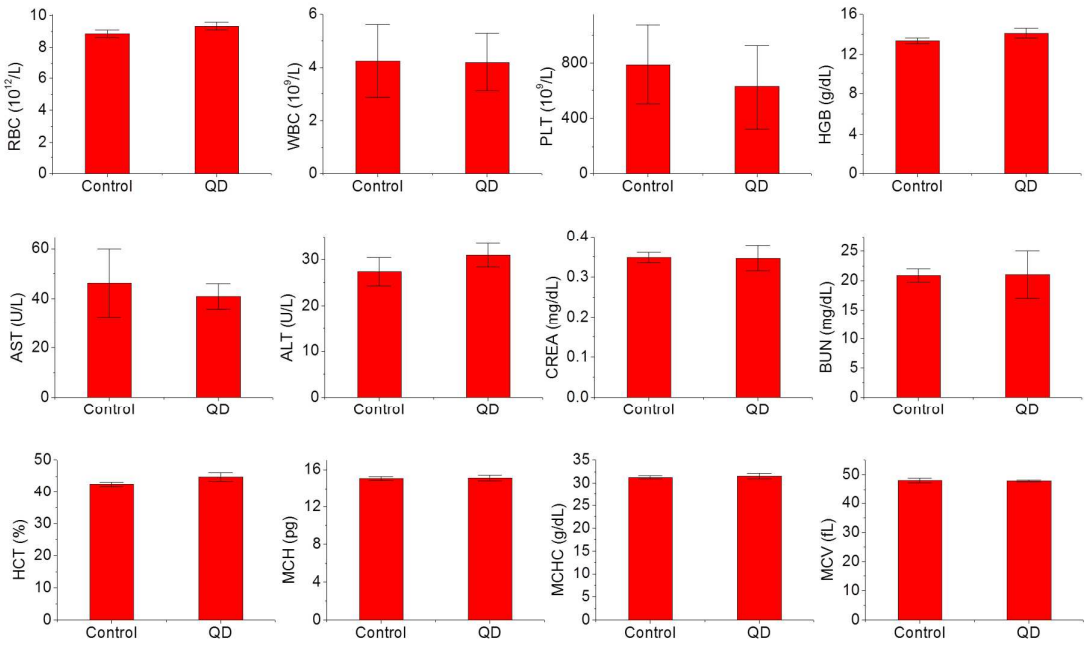

Figure S9. Toxicity studies for PA-NIRQD at small animal level. Hematological parameters and typical biochemical parameters of mice at 7 days after the intravenous administration of 0.1 nmol PA-NIRQD. RBC, red blood cell; WBC, white blood cell; PLT, platelet; HGB, hemoglobin; AST, aspartate aminotransferase; ALT, alanine aminotransferase; CREA, creatinine; BUN, blood urea nitrogen, HCT, hematocrit; MCH, mean corpuscular hemoglobin; MCHC, mean corpuscular hemoglobin concentration; MCV, mean corpuscular volume.

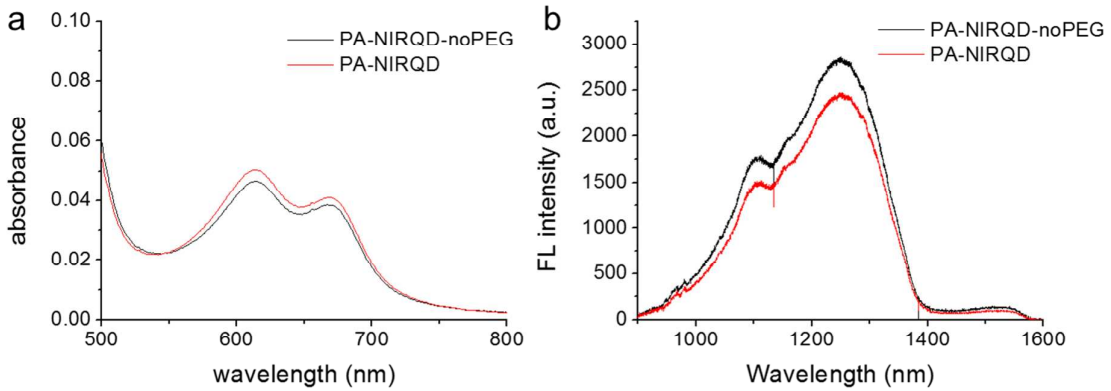

Figure S10. (a) Absorption spectra of NIRQDs conjugated with typical AcM (PA-NIRQD) and with AcM-noPEGs (PA-NIR-noPEG). (b) FL spectra of PA-NIRQD and PA-NIRQD-noPEG at the same concentration. Relative PL QYs of PA-NIRQD and PA-NIRQD-noPEG were 0.95 and 1, respectively.

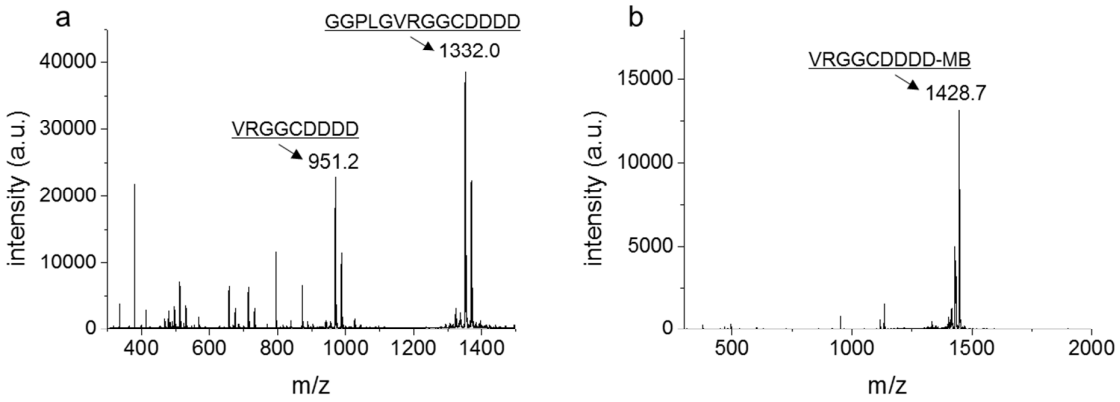

Figure S11. MALDI-TOF mass spectra of (a) MMP-2-treated AcM-noPEG that was not conjugated with MB and (b) MMP-2-treated AcM-noPEG. There was no signal of intact AcM-noPEG (GGPLGVRGGCDDDD-MB, m/z = 1810) in (b).

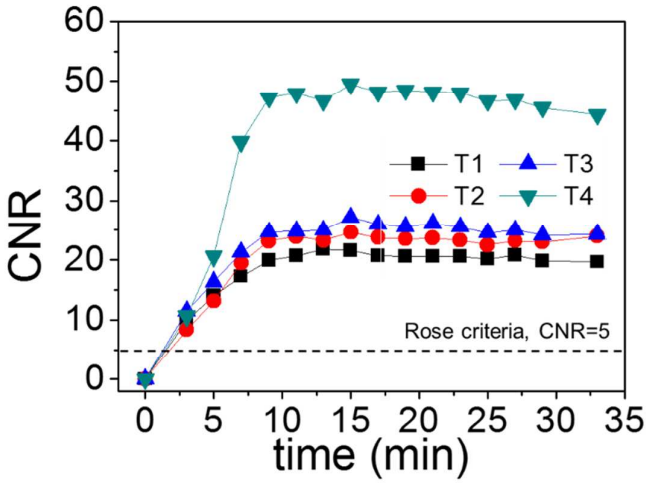

Figure S12. Time-dependent contrast-to-noise ratios (CNRs) of the selected region of T1, T2, T3, and T4 after PA-NIRQD spraying onto colon cancer.

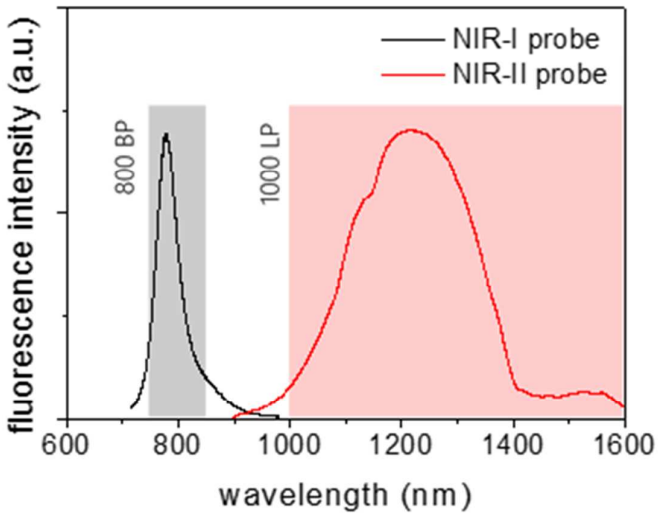

Figure S13. FL spectrum of Genhence 750 with the spectral window of an 800-nm bandpass filter (800 BP; black line). FL spectrum of NIRQDs in water with the spectral window of a 1000-nm long-pass filter (1000 LP; red line).

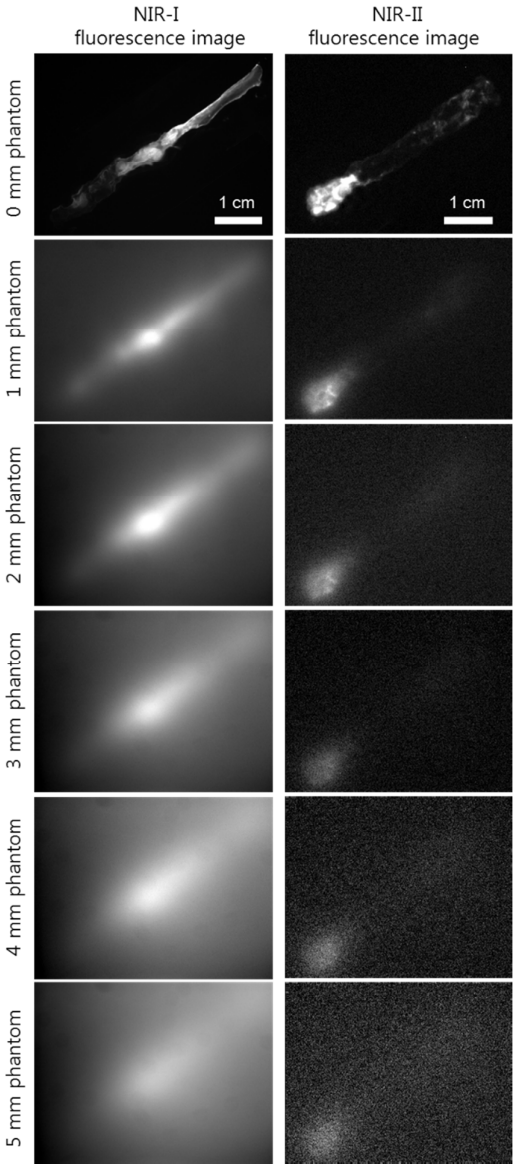

Figure S14. Tissue phantom study of Genhence 750 (NIR-I)-sprayed and PA-NIRQD (NIR-II)-sprayed colon cancers. The images are gray-scaled FL images under 1% intralipid solution (depth = 0–5 mm).

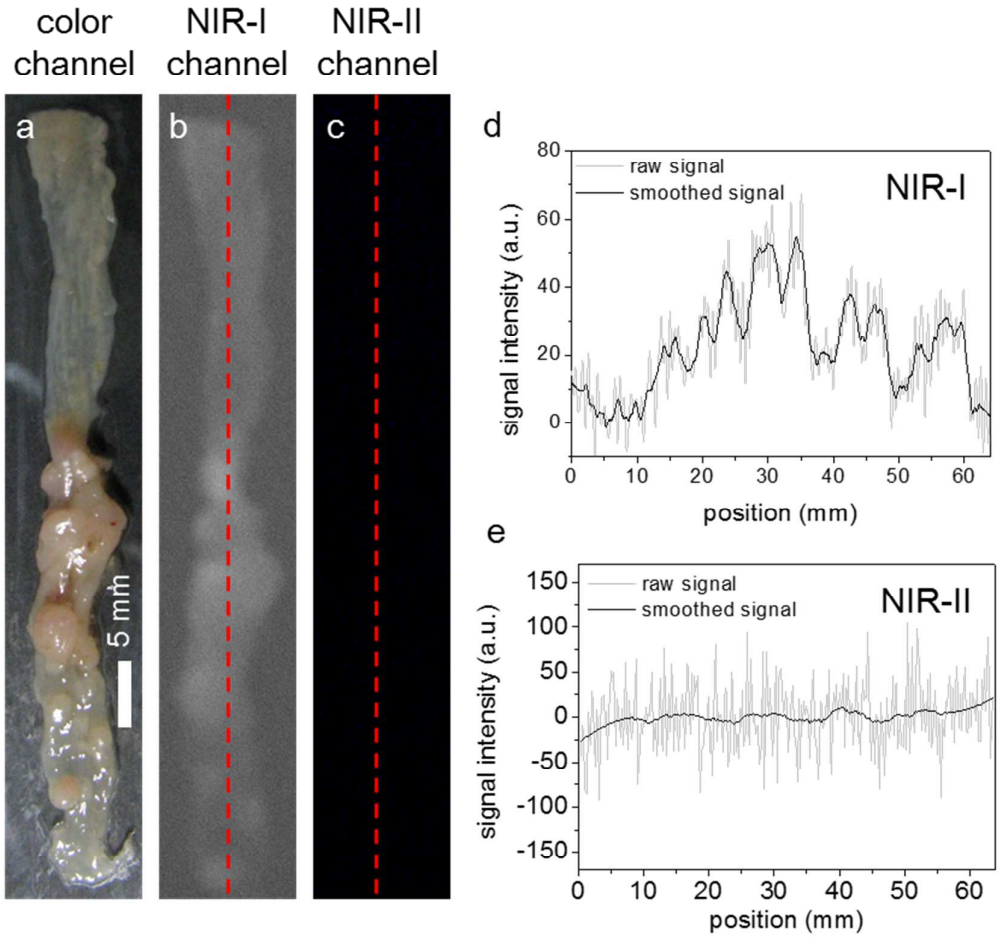

Figure S15. Autofluorescence level of intact colon in the NIR-I and NIR-II regions: (a) color image of colon cancer model and FL image of colon cancer before probe spraying in the (b) NIR-I and (c) NIR-II regions excited at 660 nm, 10 mW/cm^2 and 910 nm, 200 mW/cm^2, respectively. The NIR-I signal was detected by a Si CCD camera through an 800-nm bandpass filter, and the NIR-II signal was detected by an InGaAs CCD camera through a 1000-nm long-pass filter. The colon can be distinguished from the background in the NIR-I channel but not in the NIR-II channel. (d) and (e) FL signal profiles along the dotted red lines in the NIR-I and NIR-II channels, respectively.